Optimal control of grids and schemes for the inertial gravity waves equation

Laurent Debreu, Eugene Kazantsev

Optimal control of grids and schemes for the inertial gravity waves equation.

Laurent Debreu, Eugene Kazantsev *

Abstract

Variational data assimilation technique is applied to a simple bidimensional wave equation that simulates propagation of internal gravity waves in the ocean in order to control grids and numerical schemes. Grid steps of the vertical grid, Brunt-Vaisala frequency and approximation of the horizontal derivative were used as control parameters either separately or in the joint control. Obtained results show that optimized parameters may partially compensate errors committed by numerical scheme due to insufficient grid resolution.

1 Introduction

Contemporary ocean general circulation models are usually discretized by finite differences on a grid with rectangular cells. This discretization simplifies the model and accelerates its integration. Most oceanic numerical models use low-order space-time schemes to offer the best simplicity and efficiency. Indeed, the robustness of the scheme allows us to refine the grid keeping the computational cost constant. This possibility was considered as important during long time because the lack of resolution was the principal source of model errors.

However, advances in computer technique, ocean models are now capable to resolve finer and finer scales along both horizontal and vertical axes.

*AIRSEA, Inria Grenoble - Rhne-Alpes, LJK - Laboratoire Jean Kuntzmann, UJF - Universit Joseph Fourier - Grenoble 1, INPG - Institut National Polytechnique de Grenoble. 700, avenue Centrale 38400, Saint Martin d'Hères, France.

The direct consequence of this achievement consists in including of additional physical processes into resolved model physics. Thus, significant part of the internal gravity waves spectrum could be potentially represented by actually employed computational grids. This implies the necessity to review conventional numerical choices for the space-time integration of the model. In particular, current low-order schemes and regular grids may be responsible for dispersion errors and wrong energy transfers.

Conception of the grid and the choice of numerical scheme require, however, a special work in order to bring together somewhat contradictory needs of computational simplicity and correct reproduction of physical processes. This conception admits a certain freedom in choice of both schemes and grids. Possibility to chose the approximation order ([4]), conventional or adaptive grids [3], explicit or implicit schemes ([13]), finite elements ([2, 8]) of finite volumes ([5]) approaches are discussed and analyzed in numerous papers.

An alternative approach discussed in this paper suppose to ask the model's opinion about "optimal" discretization and scheme that will be able to compensate error committed by limited resolution of the model grid. The word "optimal" is used here in the sense of the variational control methods as numerical scheme that realizes a minimum of the specially constructed cost function.

In [10, 11], this approach has been applied to identification of lateral boundary conditions in different configurations of NEMO ([12]). It has been shown that extending the set of control variables beyond the initial value control has certain advantages that help to bring the solution closer to observations not only during the assimilation stage, but also during the forecast.

In this paper, we intend to analyse the influence of numerical schemes and grids on the model flow in a simple, academic configuration of two dimensional equation that simulates internal gravity waves in a periodical domain and to propose a way of optimization of the vertical grid and horizontal derivative approximation by variational data assimilation technique. Internal waves propagate in the oceanic interior in the water of variable density. Due to their important role in the global distribution of physical mixing and mass transport, proper representation of internal wave dynamics in numerical models is extremely important especially in modern high resolution models.

As well as in [10], tangent linear and adjoint codes, necessary for variational approach, have been obtained by the AD Tapenade described in [7]. Particular utility of automatic differentiation in the case of parameter optimization is related to the fact that the derivative of the model with respect

to internal parameters is two or three times longer (as well as in terms of the development, the number lines of the code and the necessary CPU time) than the derivative used to control the initial point of the model (see [9] for details).

2 Model setup

In order to study numerical representation of inertial gravity waves we consider a two-dimensional system proposed in [4]:

$$\frac{\partial u_q}{\partial t} + g\frac{\partial p_q}{\partial x} = 0, \quad \frac{\partial p_q}{\partial t} + \frac{1}{g\lambda_q}\frac{\partial u_q}{\partial x} = 0 \tag{1}$$

where g is the gravity acceleration. Variables u_q and p_q are supposed to be spectral coefficients in the decomposition by vertical modes $M_q(z)$ which are the eigenvectors of the Sturm-Liouville problem:

$$-\frac{\partial^2}{\partial z^2}N^{-2}\frac{\partial^2 M_q}{\partial z^2} = \lambda_q M_q, \quad \left.\frac{\partial M_q}{\partial z}\right|_{z=0} = \left.\frac{\partial M_q}{\partial z}\right|_{z=-H} = 0 \tag{2}$$

with $N(z)$ is the Brunt-Vaisala frequency that is assumed to be always positive.

Zonal velocity $u(x,z,t)$ and pressure deviation from the hydrostatic balance $p(x,z,t)$ can be calculated using coefficients u_q and p_q as

$$u(x,z,t) = \sum_{q=0}^{N-1} u_q(x,t)M_q(z), \quad p(x,z,t) = \rho g \sum_{q=0}^{N-1} p_q(x,t)M_q(z). \tag{3}$$

The influence of the numerical representation on the solution has been studied in [4]. Two principal consequences of finite dimensional discretisation of the model (1),(2) consist in wrong eigenvalues λ_q due to numerical solution of (2) and wrong approximation of the wave speed due to discrete horizontal grid.

In this paper we apply variational methods in order to correct these errors or reduce their influence on the solution. As usual, we define a set of parameters that are allowed to vary during the procedure of the minimization of the specially constructed cost function that is supposed to measure the quality of the numerical scheme. The cost function represent the weighted norm of difference between the model solutions on the high and low resolution grids.

Among these parameters we shall focus on the discretization in x coordinate of the system (1) and numerical solution of the equation (2) that is used for the spectral transformation in z coordinate. In particular, we start from the optimization of the vertical grid trying to bring the solution closer to the reference one, obtained on the high resolution grid.

We consider Charney-Philips vertical grid (fig.1) introduced in [1]

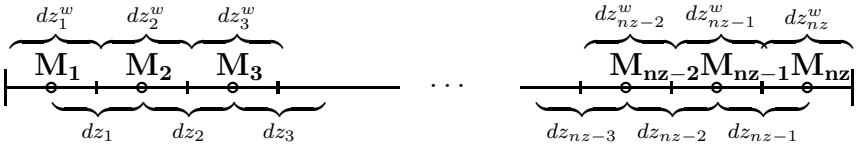

Figure 1: Vertical grid and grid step notations.

Discretized equation (2) writes on this grid

$$\begin{aligned}
\frac{N_1^{-2}}{dz_1 dz_1^w} M_1 - \frac{N_1^{-2}}{dz_1 dz_1^w} M_2 &= \lambda M_1 \\
-\frac{N_k^{-2}}{dz_{k-1} dz_k^w} M_{k-1} + \frac{1}{dz_k^w}\Big(\frac{N_{k+1}^{-2}}{dz_k} + \frac{N_k^{-2}}{dz_{k-1}}\Big) M_k - \frac{N_{k+1}^{-2}}{dz_k dz_k^w} M_{k+1} &= \lambda M_k \\
\forall k : 2 \le k \le nz-1 & \qquad (4) \\
-\frac{N_{nz-1}^{-2}}{dz_{nz-1} dz_{nz}^w} M_{nz-1} + \frac{N_{nz-1}^{-2}}{dz_{nz-1} dz_{nz}^w} M_{nz} &= \lambda M_{nz}
\end{aligned}$$

The total depth of the ocean is divided by nz intervals of equal length dz^w. We consider that eigenvectors M are defined at the middle points of each interval while their derivatives, that are related to the density and vertical velocity, are determined at the intervals boarders. Boundary conditions are prescribed at the boarders of the first and the last interval.

Numerical resolution of the system (4) approximates well eigenvectors but underestimates eigenvalues. In particular simplified case, when the Brunt-Vaisala frequency is constant, we can easily resolve the continuous problem (2) and get:

$$\lambda_k^{theor} = \Big(\frac{\pi(k-1)}{N\ H}\Big)^2, \quad M_k^{theor} = \cos\Big(\frac{\pi(k-1)z}{H}\Big)$$

Comparison avec numerical solution of (4) shows that all eigen vectors are approximated with the precision of the floating point arithmetics, but largest eigenvalues of (4) have much lower values than corresponding theoretical

ones. An example for the resolution $nz = 51$ is shown in fig.2A (two lower lines corresponding to the constant N). One can see that the square root of the largest numerically calculated eigenvalue is 1.5 times lower than its theoretical estimates. So far, λ participates explicitly in the system (1) and determinates the wave velocity of the mode M_q as $c_q = 1/\sqrt{\lambda_q}$, we can estimate the numerical error due to discretization in the vertical coordinate z committed in the solution of (4)

$$\delta c_q = \sqrt{\frac{\lambda_k^{theor}}{\lambda_k^{num}}} \tag{5}$$

In the more complex configuration, we consider a variable Brunt-Vaisala frequency N which is defined by the hyperbolic profile

$$N = N(z) = \frac{-2m/s}{z - 200m} \text{ where } -4000m \leq z \leq 0. \tag{6}$$

This formula allows N to vary from $5 \times 10^{-4} s^{-1}$ at the first node near the bottom to $1 \times 10^{-2} s^{-1}$ at the last node near the surface. In this case, eigenvalues can not be obtained theoretically and approximations of exact values are calculated on the five times finer grid. First 51 of total 251 eigenvalues are considered as the reference ones. The comparison of the reference and numerically calculated eigenvalues on the coarse grid is also shown in fig.2A (two upper lines corresponding to the variable N). As one can see in this plot, the variable N slightly increases the reference eigenvalues and completely modifies the error committed on the coarse grid. The error changes sign and the square root of the largest numerical eigenvalue becomes two times bigger than the reference one.

In addition to the error induced by the vertical discretization, the wave speed is also perturbed by finite resolution in x coordinate. If we substitute a wave $u = e^{i\pi(\omega t + kx)}$ into the equation (1), we get the dispersion relationship: $\omega/k = c = 1/\sqrt{\lambda_q}$. However, if we apply a numerical scheme in order to discretize this equation in x, we get another dispersion relationship. Thus, if we use leap-frog scheme for the discretization in time and some central-differences for derivatives in x

$$\frac{u_{i,q}^{n+1} - u_{i,q}^{n-1}}{2\tau} = -g\frac{c_u^1 p_{i-2,q}^n + c_u^2 p_{i-1,q}^n + c_u^3 p_{i,q}^n + c_u^4 p_{i+1,q}^n}{h}$$

$$\frac{p_{i,q}^{n+1} - p_{i,q}^{n-1}}{2\tau} = -\frac{1}{g\lambda_q}\frac{c_p^1 u_{i-1,q}^n + c_p^2 u_{i,q}^n + c_p^3 u_{i+1,q}^n + c_p^4 u_{i+2,q}^n}{h} \qquad (7)$$

that realizes either second (with $c = 0, -1, 1, 0$) or fourth (with $c = 1/24$, $-27/24, 27/24, -1/24$) order approximation of the derivative, we get approximated dispersion relationships

$$\omega_2 = \frac{\arccos((4\tau^2\cos(\pi kh) + \lambda h^2 - 4\tau^2)/(\lambda h^2))}{2\pi\tau}$$

$$\omega_4 = \frac{1}{2\tau} - \frac{\arccos\frac{54\tau^2\cos(2\pi kh) - \tau^2\cos(3\pi kh) - 783\tau^2 cos(\pi kh) - 144\lambda h^2 + 730\tau^2}{144\lambda h^2}}{2\pi\tau}$$

Corresponding wave velocities $c = \omega/k$ are shown in fig.2B for the resolution $nx = nz = 51$ assuming that the eigenvalue λ is equal to one. We see that both numerical approximations of the horizontal derivative underestimate the wave velocity. Consequently, we can state that numerically calculated eigenvalues λ_q in the case $N = const$ increase the velocity c_q when q increases while the discretization in x results in a lower velocity with bigger k. This fact ensures the existence of appropriate k and q for which errors in wave velocity are compensated by each other.

However, the numerical wave velocity remains wrong for other combinations of k and q and the wave becomes either too slow for big k and small q, or too rapid for small k and big q. In the case of variable N, both numerical errors slow the wave speed down and numerical errors committed in x and z discretizations enhance each other.

In order to obtain an optimized wave speed for the particular composition of different waves determined by initial conditions, we shall solve a variational problem trying to minimize a cost function that measures the distance between a numerical solution and a presumably exact one.

We construct the cost function for the system (1) as

$$\mathcal{J} = \sum_{n=1}^{nt}\sum_{k=1}^{nz}\sum_{i=1}^{nx}\Big((u_{i,k}^n - \bar{u}_{i,k}^n)^2 + (p_{i,k}^n - \bar{p}_{i,k}^n)^2\Big) \qquad (8)$$

where $\bar{u}$ is supposed to be the reference model solution, obtained on a much finer grid. The sum is made in the physical space z rather than in over all vertical modes q.

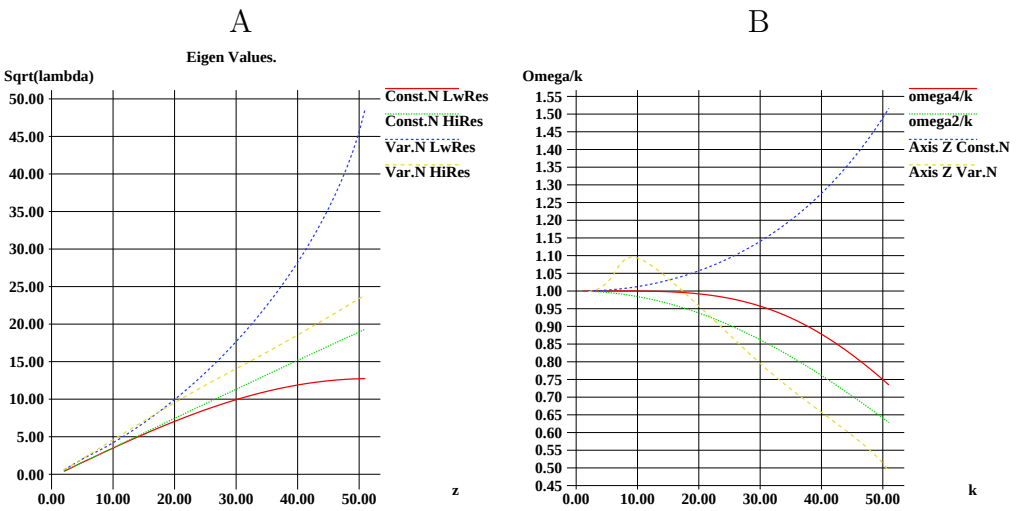

Figure 2: Square roots of exact and caclulated eigenvalues (2) for cases with constant and variable Brunt-Vaisala frequency N (A) and the numerical error in the wave speed (B)

To search for a minimum of the cost function, we use its gradient with respect to control parameters. Tangent and adjoint models necessary to calculate the gradient, have been automatically generated by the Tapenade software presented in [7]. This software analyses the source code of the model and produces the codes of the tangent model and of its adjoint. The minimization procedure used in all experiments below is based on the limited memory quasi-Newton method [6].

We perform either a separate or a joint control of the discretizations in both x and z directions. We consider the cost function (8) that is supposed to depend on the set of parameters to be optimized. Among parameters in this set we try to use the following

- grid steps in the vertical discretisation dz_k, dz_k^w used in the Sturm-Liouville problem (4),
- Brunt-Vaisala frequency N_k that is supposed to be known with a limited accuracy and allowed to vary within these limits,
- coefficients c_1, c_2, c_3, c_4 in the approximation of the horizontal derivative in (7),

- joint optimization of all parameters above.

We do not intend to optimize gravity acceleration g assuming it is known exactly, nor parameters of time forwarding scheme.

The problem (7), (4) is considered in a square box of $L = 500$ km length and $H = 4$ km depth with periodical boundary conditions in x and Neumann conditions (see (2)) in z. The square is discretized with a regular low-resolution grid that counts $nx = 102, nz = 51$ nodes. Time step is equal to $\tau = 24$ minutes.

Two kinds of starting points are considered: just two distinctive modes in x and in z

$$\begin{aligned} u(x,z,0) &= 1.6 \times 10^{-5} \cos(16\pi x/L) \cos(2\pi z/H) \\ p(x,z,0) &= 4.2 \times 10^{-2} \sin(6\pi x/L) \cos(7\pi z/H) \end{aligned} \tag{9}$$

or a more complex composition of long waves:

$$\begin{aligned} u(x,z,0) &= \sum_{K_x=1}^{8} \sum_{K_z=1}^{12} \frac{4 \times 10^{-3}}{\sqrt{K_z K_x}} \cos(2K_x \pi x/L) \cos(K_z \pi z/H) \\ p(x,z,0) &= \sum_{K_x=1}^{8} \sum_{K_z=1}^{12} \frac{0.5}{\sqrt{K_z K_x}} \sin(2K_x \pi x/L) \cos(K_z \pi z/H) \end{aligned} \tag{10}$$

The first kind of initial conditions (9) ensures two separate frequencies clearly visible on the energy evolution plot in fig.3. One of them, with period

$$\frac{L\sqrt{\lambda_7}}{3 \times 86400} = 5.3 \text{ days},$$

corresponds to the wave defined by initial conditions for p, the other one, with period

$$\frac{L\sqrt{\lambda_2}}{8 \times 86400} = 0.57 \text{ days},$$

is determined by $u(t = 0)$.

The second kind represents a sum of waves which length exceeds $L/8$ in x and $H/6$ in z. These waves are weighted to ensure lower contribution of shorter waves. This initial point provides a solution with numerous waves moving with different wave velocities as shown in fig.4.

As the most complex configuration we consider the same sum of multiple waves in the initial state accompanied by variable Brunt-Vaisala frequency N which is defined by a hyperbolic profile (6).

We don't introduce short waves in the solution supposing that a model with more realistic physics would dissipate these waves.

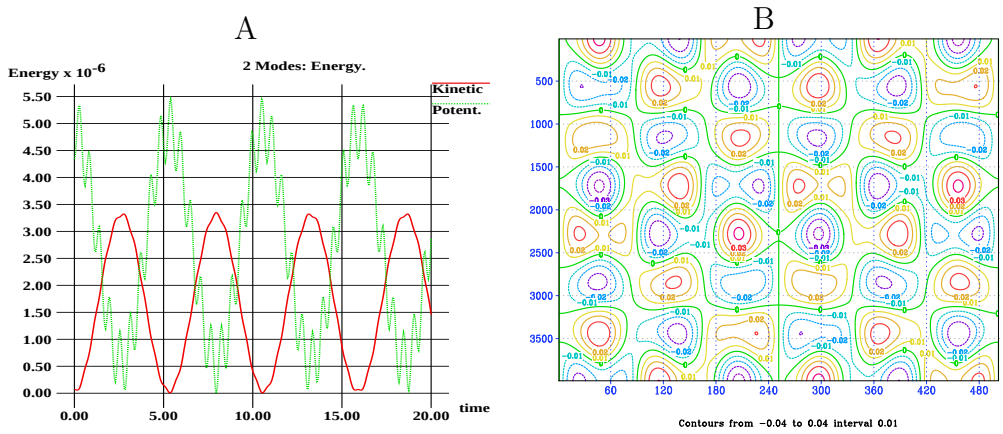

Figure 3: Two modes: evolution of energy from the starting point (9) (A) and the field of $p(x, z, t = 20 \text{ days})$ (B)

The reference data $\bar{u}, \bar{p}$ for the cost function (8) have been generated by the same model on the 5 times finer grid $nx = 502, nz = 255$. These dimensions of the fine grid ensure that for any node of the coarse grid there exists a node on the fine grid at the same position. This allows us to avoid interpolations and to calculate the cost function (8) performing the sum over all nodes of the coarse grid taking $\bar{u}, \bar{p}$ at the corresponding nodes of the fine grid.

Assimilation window in chosen as 20 days, that corresponds approximately 4 periods of the wave, initiated by (9). In order to see the behavior of the solution beyond the assimilation window, the cost function value calculated over 200 days period is also examined. This is particularly important when the composition of waves prescribed in the initial conditions has a longer period of the resulting wave than the assimilation window.

Several assimilation experiments are performed for the model with these two kinds of initial points with different controlled parameters. Equally spaced x and z grids with either second or fourth order approximation of derivatives are considered as initial guess in all minimization experiments. The cost function (8) value after 100 iterations is shown in the table 1. Experiments with more iterations have been performed with no significant improvement of results.

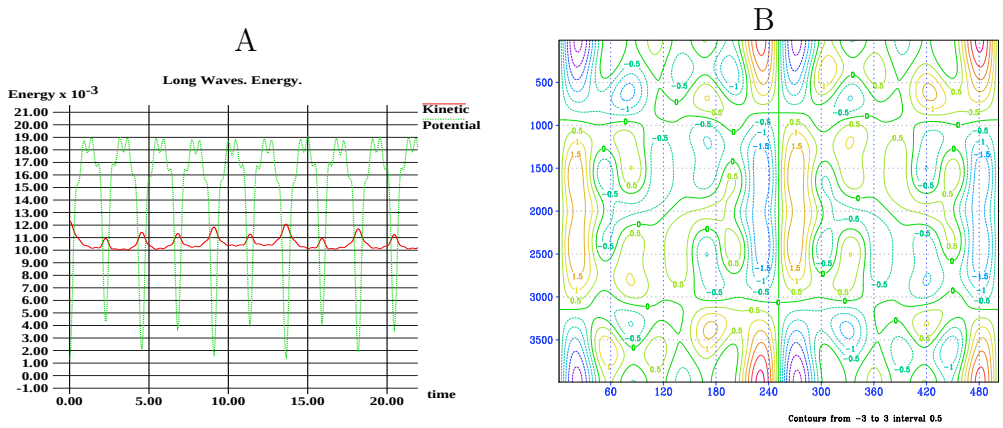

Figure 4: Set of long waves: evolution of energy from the starting point (10) (A) and the field of $p(x, z, t = 20 \text{ days})$ (B)

One can see that in the conventional configuration, fourth order approximation provides a solution that is slightly closer to the reference high resolution one. The principal source of the error lies in the difference of the wave speeds, that's why the fourth order approximation gives better results on the 20 days interval: the second order scheme has already induced the significant phase difference between the reference and approximated solutions while the fourth order scheme succeeded to keep a small phase difference. However, on the long time interval the phase difference becomes bigger that gives comparable cost function values obtained with both schemes.

Optimization of the vertical grid (either grid steps or Brunt-Vaisala frequency) improves the solution in the simple case of evolution of two modes. The trajectory on the low-resolution grid becomes indistinguishable from the reference one due to exact compensation of errors in the two wave speeds of each mode. However, in a more complex case of multiple modes, partial compensation of numerical errors is only possible on a short time interval within the assimilation window. Out of the window, low resolution model with second order approximation of the spatial derivative and optimized vertical grid exhibits even bigger cost function value than on the conventional grid. Better results can be obtained optimizing vertical grid with fourth order derivative approximation. The cost function on the long interval is reduced, however, 8 times with respect to conventional grid.

Optimizing the coefficients of horizontal derivative discretization helps us

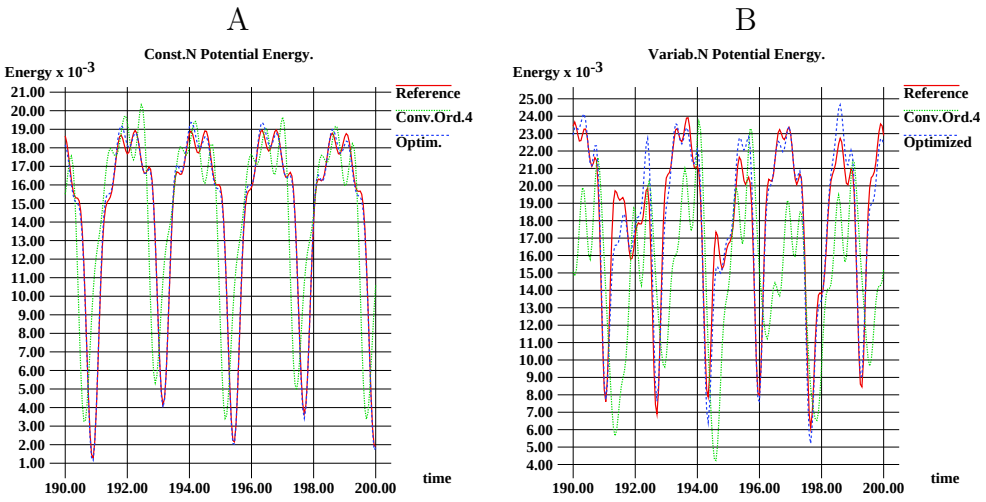

Figure 5: Potential energy of the reference model, conventional and all-optimized schemes in cases of the constant (A) and variable N (B).

to get the solution that exactly coincides with the reference one in the case of propagation of two waves. In the case when multiple waves exist in the initial conditions, the cost function is also reduced, but remains bigger than with optimized vertical grid.

Better result is obtained in the joint optimization of both vertical grid steps and derivative approximation. The cost function shows lowest values as within the assimilation window and beyond the window.

Similar situation is observed in the case with variable N. Optimization of the vertical grid provides lower cost function than optimization of the horizontal derivative. The lowest value is also obtained in the joint control of all parameters.

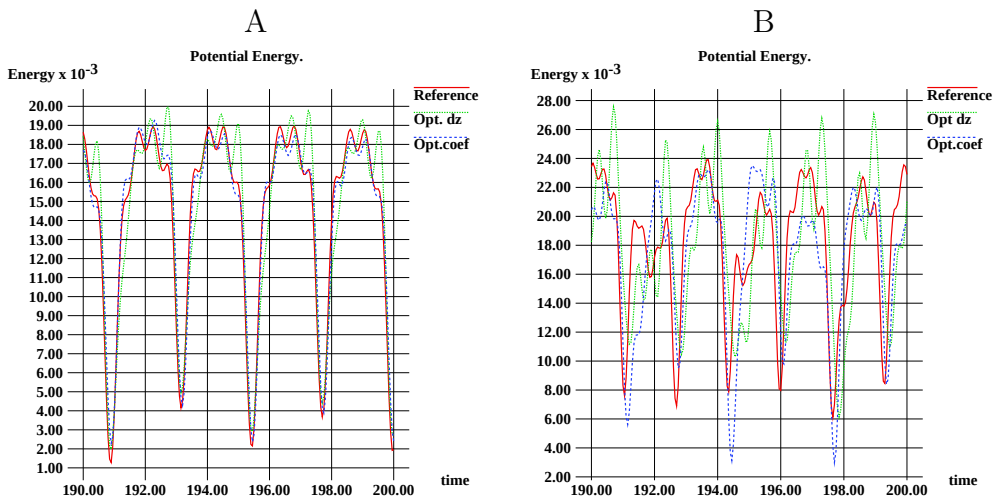

Figure 6: Potential energy of the reference model, optimized vertical grid and optimized coefficients c_m schemes in cases of the constant (A) and variable N (B).

Table 1. Cost function $\mathcal{J}$ (8) with conventional and optimized schemes.					
Exp.	Order	Two Modes		Set of Long Waves	
		$\mathcal{J}(20)$	$\mathcal{J}(200)$	$\mathcal{J}(20)$	$\mathcal{J}(200)$
Conventional	2	1.85×10^{-1}	19.4	560.2	98 847
Opt. dz, dz^w	2	5.43×10^{-5}	6.10×10^{-4}	161.1	114 287
Opt. N	2	4.45×10^{-4}	6.30×10^{-3}	164.0	115 591
Conventional	4	1.89×10^{-2}	16.7	54.86	42 099
Opt. dz, dz^w	4	9.19×10^{-7}	9.31×10^{-6}	5.58	4 447
Opt. N	4	7.07×10^{-5}	1.58×10^{-3}	7.42	5 606
Opt. c_m	-	0	0	15.74	11 752
Opt. dz, dz^w, N, c_m	-	0	0	3.40	2 453
Variable Brunt-Vaisala frequency N					
Conventional	4	–	–	478.4	70 754
Opt. dz, dz^w	4	–	–	23.1	29 759
Opt. c_m	-	–	–	376.9	60 172
Opt. dz, dz^w, N, c_m	-	–	–	7.75	15 635

The influence of the optimization can be viewed on the potential energy plot showed on fig.5. We plot the evolution during the last 10 days (between 190th and 200th days) for three model runs: the reference trajectory of

the high resolution model, low resolution model with conventional vertical grid and fourth order approximation of the horizontal derivatives and low-resolution model with optimized both vertical grid, Brunt-Vaisala frequency and derivatives.

In the case of the constant N, long waves approximated on the conventional grid are a little faster than the reference ones (see fig.2B) due to numerical error in eigenvalues which is not completely compensated by horizontal derivative approximation. This results in the displacement to the left of peaks of energy. Contrary to that, variable N ensures smaller numerical wave velocity (eigenvalues λ are overestimated in this case) and the peak of energy are moved to the right with respect to the high resolution reference trajectory. One can see that for both constant and variable N the variational method has succeeded to compensate the error in the wave speed and all peaks of the potential energy coincide with the reference ones. Unfortunately, variational control does not allow to compensate the error in the peaks amplitude, that explains a non-null final cost function value in all experiments.

We should note, that separate optimization of the vertical grid or coefficients for the derivative in x does not allow to retrieve the reference wave speed. This is illustrated in fig.6 where the potential energy for trajectories on the optimized vertical grid and optimized coefficients c_m schemes in cases of the constant (A) and variable N are compared with the reference solution during the same time interval as in fig.5. One can see, in the experiment with constant N (fig.6A) even the optimized vertical grid shows the solution with a little bit faster waves than the reference while the waves produced by the model with optimized c_m are too slow. In the experiment with variable N (fig.6B), both optimizations result in lower wave speed with respect to the reference one.

To illustrate the the evolution of two-dimensional fields we plot the $p(x, z, t =$ 200 days) obtained in the most complex case with variable N in fig.7. Three fields are compared: obtained by the reference high resolution model fig.7A, by the optimized model on the coarse grid (B) and by the model on low resolution conventional grid (C). One can see that spatial pattern of the optimized solution is quite close to the reference one, but the waves amplitude is not sufficient to fit the solution on the fine grid. Low resolution model without optimization exhibits both insufficient amplitude and wrong spatial pattern.

Optimized coefficients of approximation of the horizontal derivative a

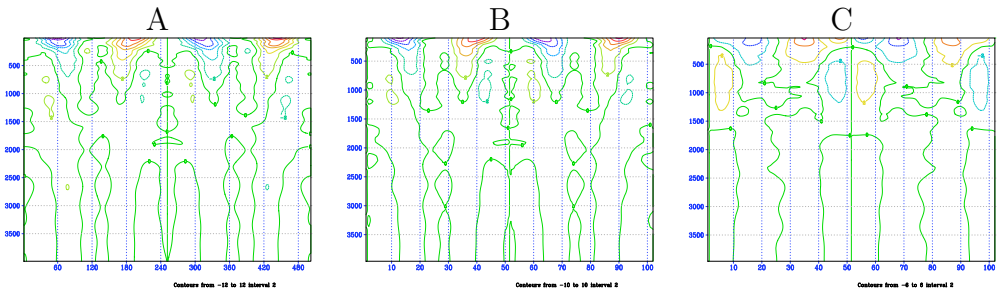

Figure 7: Final (t=200 days) p field in simulations with variable N: reference high resolution (A), low resolution with optimised parameters (B) and low resolution with conventional scheme (C).

shown in the table 2. One can see that only a little modification with respect to a conventional fourth order scheme is made by the optimization. All coefficients sets approximate the derivative multiplied by some coefficient rather than the derivative itself. Significant difference between optimized and conventional coefficients is observed in cases of variable N and two modes evolution.

To understand this phenomenon, we calculate the modifications of the wave speed imposed by the optimized schemes and plot them in fig.8. Taking into account that the solution contains long waves only, we restrict the plotting area by low wave-numbers.

One can see the principal influence of the optimization on the resulting wave velocity. In the simplest case of two modes evolution, coefficients c have undergone the strongest modification. This fact can be explained by comparison of two figures: fig.8 and fig.2. The purpose of the optimization is to compensate the wave speed error committed by numerical approximation (4). Errors in just two eigenvalues λ_2 and λ_7 require a correction in this case. It becomes to be possible: modified approximation of the horizontal derivative reduces the wave speed at $K_x = 3$ to compensate an excessive speed determined bu numerical λ_7 and keeps the wave speed at $K_x = 8$ close to the exact speed because numerical λ_2 is also close to the analytical value. The consequence of that is the vanishing value of the cost function with optimized approximation of the horizontal derivative.

When multiple long waves are presented in the initial point and N is constant, optimization choose to slightly reduce the speed for all wave-numbers

in order to compensate the error of numerically calculated eigenvalues. In the case of variable Brunt-Vaisala frequency N, the error in the wave velocity due to λ is more important for long waves (see fig.2B), that's why the slowing the waves down by the optimized derivative in x is more important also.

Table 2. Optimized coefficients c_m in (7).				
Conventional fourth order approximation				
	1.125	-1.125	-0.0417	0.0417
Two Modes, Optimized c_m				
c_u	1.292	-1.292	-0.103	0.103
c_p	1.110	-1.110	-0.037	0.037
Long waves, Const. N, Optimized c_m				
c_u	1.110	-1.110	-0.038	0.038
c_p	1.114	-1.114	-0.038	0.038
Long waves, Const.N, Optimized all param.				
c_u	1.102	-1.102	-0.038	0.038
c_p	1.110	-1.110	-0.036	0.036
Long waves, Var. N, Optimized all param.				
c_u	1.059	-1.059	-0.033	0.033
c_p	1.100	-1.100	-0.032	0.032

Results of optimization of the vertical grid are shown in fig.9. One can see quite different modification of the grid steps. In the case of constant frequency N, multiple nodes of the vertical grid are displaced to several meters from their initial position. The nodes displacement reaches 14 meters near the bottom and near the surface of the ocean where the grid become coarser.

In the case of variable N, the grid steps are modified near the surface only. The first grid cell of the w grid (see fig.1) double its initial length displacing the second node deeper in the ocean while the node of the M grid is moved toward the surface.

Control of the Brunt-Vaisala frequency gives a similar results. Resulting cost function values are quite close after separate optimizations as grid steps and N. Joint control of these two sets of parameters does not improve the results. It is obvious because the increasing of parameters number does not increase the number of controlled degrees of freedom. Optimizing one of them or another one we control the same coefficients in the problem (4) and get the same modification of the eigenvalue problem. Optimized frequency

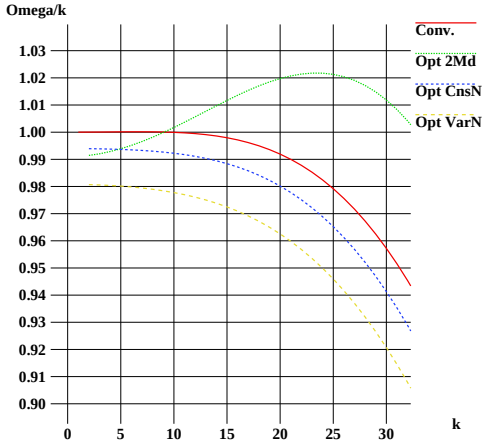

Figure 8: Wave velocities defined by conventional and optimized derivative discretizations.

in experiments with simple control of N is not shown because it has the same pattern as optimized grid steps.

It should be noted that joint or separate control of vertical grid steps and the Brunt-Vaisala frequency results in a small modification of the eigenvalues themself. The control of parameters of the Sturm-Liouville problem (4) influences principally on the eigenvectors and especially on the second half of them corresponding to largest eigenvalues.

3 Conclusion

We have applied variational control methods to optimization of the vertical grid and numerical scheme of the simple bidimensional wave equation that simulates propagation of internal gravity waves in the ocean. Grid steps of the vertical grid, Brunt-Vaisala frequency and approximation of the horizontal derivative were used as controlled parameters either separately or in the joint control. Obtained results show that optimized parameters may partially compensate errors committed by numerical scheme due to insufficient grid resolution.

Optimal vertical grid steps and coefficients in horizontal derivative approximation found in the variational control procedure allow us to get the

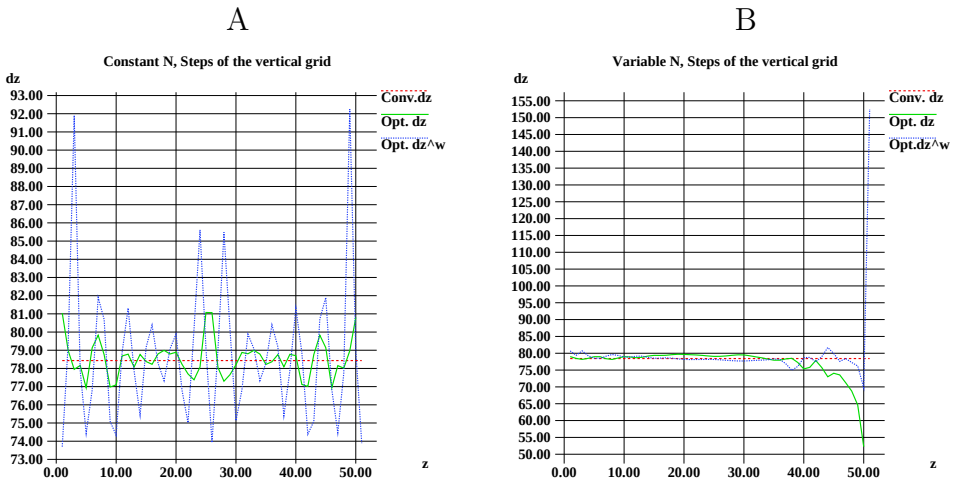

Figure 9: Optimized grid steps of the vertical grid in experiments with the constant (A) and variable N (B).

model solution that is rather close to the solution of the reference model. The error in the wave velocity on the coarse grid is mostly compensated in experiments with joint control of parameters while the error in the wave amplitude occurs to be more difficult to correct.

Separate optimization of either horizontal or vertical parameters seems to be less efficient. The wave speed can be corrected in simple cases when few modes are present, but remains wrong in more complex cases with numerous modes in the solution or variable frequency N.

We can note also the importance of using of high order schemes for discretization of spatial derivatives in the optimization experiments. As it is shown in the table 1, if the horizontal derivative is approximated with the second order, optimization of the vertical grid leads to bigger cost function value on long time scales.

Optimization of the horizontal derivative gives us a numerical scheme that does not approximate a derivative. In general, some coefficient appears in front of the derivative to modify the wave velocity when it is necessary to compensate its excess due to underestimated eigenvalues of the Sturm-Liouville problem (2).

Analyzing optimal grid steps of the vertical grid, we can see that they may be in a disagreement with requirements of other model physics. Thus,

bigger grid steps near the bottom correspond in general to conventional grids used in ocean circulation models because deep ocean currents are slow laminar. However, coarser grid near the surface, obtained in the optimization procedure, is in evident contradiction with the necessity to finely resolve the surface boundary layer. Consequently, additional analysis of obtained optimized parameters from the point of view of they agreement with the model is necessary.

References

[1] J. G. Charney and N. A. Phillips. Numerical integration of the quasi-geostrophic equations for barotropic and simple baroclinic flows. *Journal of Meteorology*, 10(2):71–99, 1953.

[2] S. Danilov, G. Kivman, and J. Schroter. A finite-element ocean model: principles and evaluation. *Ocean Modelling*, 6(2):125 – 150, 2004.

[3] Laurent Debreu, Christophe Vouland, and Eric Blayo. AGRIF: Adaptive Grid Refinement in Fortran. *Computers and Geosciences*, 34(1):8–13, January 2008.

[4] Jérémie Demange, Laurent Debreu, Patrick Marchesiello, Florian Lemarié, and Eric Blayo. Numerical representation of internal waves propagation. Research Report RR-8590, INRIA, September 2014.

[5] Darren Engwirda, Maxwell Kelley, and John Marshall. High-order accurate finite-volume formulations for the pressure gradient force in layered ocean models. *Ocean Modelling*, 116:1 – 15, 2017.

[6] J.C. Gilbert and C. Lemarechal. Some numerical experiments with variable storage quasi-newton algorithms. *Mathematical programming*, 45:407–435, 1989.

[7] L. Hascoët and V. Pascual. Tapenade 2.1 user's guide. Technical Report 0300, INRIA, 2004.

[8] N.G. Iakovlev. On the simulation of temperature and salinity fields in the arctic ocean. *Izvestiya, Atmospheric and Oceanic Physics*, 48(1):86–101, 2012.

[9] E. Kazantsev. Optimal boundary discretisation by variational data assimilation. *Int. J. for Numerical Methods in Fluids*, 65(10):1231–1259, 2011.

[10] E. Kazantsev. Optimal boundary conditions for orca-2 model. *Ocean Dynamics*, 63(8):943–959, 2013.

[11] E. Kazantsev. Optimized boundary conditions at staircase-shaped coastlines. *Ocean Dynamics*, 65(1):49–63, 2015.

[12] G. Madec and the NEMO team. Nemo ocean engine. Technical Report 27, Note du Pôle de modélisation de l'Institut Pierre Simon Laplace, 2012.

[13] Alexander F. Shchepetkin. An adaptive, courant-number-dependent implicit scheme for vertical advection in oceanic modeling. *Ocean Modelling*, 91:38 – 69, 2015.